British Journal of Applied Science & Technology
3(4): 860-883, 2013

SCIENCEDOMAIN *international*
www.sciencedomain.org

Analytical Technique for Predicting Passenger Car Gearbox Structure Noise Using Vibration Response Analysis

Shawki S. Abouel-Seoud[1], Eid S. Mohamed[1*], Ahmed A. Abdel-Hamid[1] and Ahmed S. Abdallah[1]

[1]Automotive Engineering Department, Faculty of Engineering, Helwan University, Egypt.

Authors' contributions

This work was carried out in collaboration between all authors. Author SSA designed the study, performed the statistical analysis, wrote the protocol, and wrote the first draft of the manuscript and managed literature searches. Authors ESM, AAA, ASA managed the analyses of the study and literature searches. All authors read and approved the final manuscript.

Research Article

Received 13th February 2013
Accepted 6th May 2013
Published 1st June 2013

ABSTRACT

The gear pair assembly remains one of the major noise and vibration sources in power transmission systems typically used in automotive, aerospace and industrial applications. The gearbox structure vibration and noise signatures are often dominated by several high-level tonal peaks that occur at the fundamental gear mesh frequency and its harmonics and other sources. In this paper, development of the concept of a method for predicting the contributions to exterior noise radiated by an original vehicle gearbox structure using measured vibration response. An idealization of the gearbox surface as a set of flat plates was used to calculate the radiation efficiency from physical properties and edge (end) constraints of each plate, and the vibration response of the gearbox structure surface was measured using accelerometers. These data were used in a simple acoustical power theory to determine 1/3-octave band sound pressure level under free field conditions for the whole and individual noise sources. Moreover, the prediction of the individual noise sources in order to pinpoint the exact problem area in the gearbox structure so that treatment or redesign can be carried out in correct way.

**Corresponding author: E-mail: eng_eid74@yahoo.com;*

Keywords: Idealization; vibration velocity; noise, radiation efficiency; accelerometers; air density; predicted sound pressure; 1/3-octave band; frequency.

a_i	area of i plate (panel) in the idealization	m^2
A	area of set of panels	m^2
ρ	density of air	$Kg.m^{-3}$
C	speed of sound in air	$m.s^{-1}$
P	acoustic pressure	$N.m^{-2}$
S	area of a surface in a defined acoustic field = 2πr for free field conditions	m^2
r	distance from a point on a hypothetical surface in space and source = 0.6	m
V	mean square time and space average velocity	$m.s^{-1}$
α	panel area ratio	
γ	wave number ratio	
$F_{m,n}$	fundamental natural frequency of panel	Rad. s^{-1}
E	Young's modulus	$N.m^{-2}$
a, b	panel dimensions (X,Y)	m
W_{rad}	radiated acoustic power	W
σ	radiation efficiency	
ν	Poisson's ratio	
$W_{vib.}$	vibration power	W
t	panel thickness	m
pρ	density of panel material	Kg.m-3
m, n	Number of 1/2- sine wave along sides a, b (modal number)	
I	sound intensity	W.m-2
γ	non-dimensional wave number ratio	
K	acoustic wave number	m-1
Kp	structure wave number	m-1

1. INTRODUCTION

The relationship between the meshing phase difference and rotational vibration of planet gears was investigated from the stand point of their rotational meshing cycle [1]. Using planetary gear sets with and without phase difference, measurements were made of their noise and vibration acceleration under varying driving conditions. The method of finishing of the gear, the tooth profile contact ratio and other factors were varied in order to compare and analyze the measured data. An original planetary gear set testing machine was designed and built so planetary gear sets in four-speed automatic transmission fitted on production vehicles was tested separately in each speed range. Planetary gear sets were tested under varying rotational speeds and tooth face loads to examine how vibration and noise were affected by different methods of finishing the test gears, different contact ratios and other factors. It was shown that the noise and vibration levels of a planetary gear set with a meshing phase different can be further reduced by improving gear accuracy and tooth face roughness.

Some dynamical effects of adding a certain amount of noise in a theoretical model for rattling in single-stage gearbox systems with a backlash, consisting of two wheels with a sinusoidal driving were investigated, where extrinsic noise was unavoidable in laboratory and industrial contexts. One of the outstanding features, a phenomenon called basin hopping was described, which consists of the intermittent switching between two or more basins of

attraction, when the system was subjected to noise. Basin hopping was conspicuous, in particular, when the basin boundaries were fractal. In practice basin hopping can be highly undesirable and even dangerous, since it may produce large amplitude jumps in the motion of the gear wheels and a consequent fatigue of the material, if not the complete collapse of the gearbox while in operation [2].

An experimental study of the rattle noise phenomenon is realized on a simplified gearbox and allows the assess of the validity of a simple model as Kelvin–Voigt applied to rattle noise. A test rig has been designed to produce rattle phenomenon under a perfectly controlled excitation and equipped to achieve acoustic and vibratory measurements. One specification of the test rig was to impose to the gearbox input shaft an acyclism not only sinusoidal but composed of several harmonics with relative amplitudes and phases were adjustable at will, which allows a very precise measurement of the gearing dynamics. An interested in the rattle threshold (i.e. excitation conditions imposed to gearbox that cause rattle to occur) have been obtained and in the influence of excitation parameters and geometrical gearbox parameters on rattle. About rattle threshold, iIt was proved that, for a constant gearbox configuration, threshold was, at first, linked to the kinetic energy imposed to the input shaft of the gearbox. In other words, the spectral composition of the acyclism had little influence. Threshold was increased when backlash was increased and was decreased when the unloaded gear was increased [3].

The reduction of rattle noise was optimized for a 5 speed gearbox based on a torsional vibration model formulated. The Rattle noise is calculated and simulated based on the design parameters, where all pinion and wheel gears are helical. Through simulation, it was concluded that increasing the geometric parameters of the gearbox, such as the module and number of teeth results in increased rattle noise. In addition, increased axial clearance results in increased rattle noise until the axial clearance reaches its maximum value, then the rattle noise decreases. Moreover, increased backlash causes decreased in rattle noise until the backlash reaches its maximum value, then the rattle noise increases. Changing the helix angle resulted in different levels of rattle noise, while changing the face width resulted in a constant level of rattle noise. Furthermore, increasing the gearbox operational parameters, such as the angular acceleration and excitation frequency, caused increased gearbox rattle noise. Some geometric design parameters, such as the module, and number of teeth must satisfy desired safety protocols, and some backlash are necessary to allow room for an oil film for all conditions of thermal expansion and contraction [4].

A formulated free damped model was presented to study gear vibrations. The model was excited by repeated teeth impact at each entrance of teeth into the meshing-singular process. At the moment of teeth entrance into the mesh, teeth impact occurs, and excites free vibration. Apart from stiffness fluctuation, teeth impacts also excite dynamic forces, vibration and noise. The calculations were based on singular systems theory and on measurement. The internal dynamic forces in teeth mesh, vibration and noise are consequences of the same causes. These causes are: change in teeth deformation, teeth impact, gear inertia due to measure and teeth shape deviation, etc. The results of that model well approximate the measured in all the three frequency ranges which are the sub critical, resonant and supercritical [5].

The structural vibration and the associated acoustic radiation of a simplified gearbox was numerically studied. A FE formulation was developed for modeling the dynamic behavior of the interior coupled acoustic-structural system. The effect of the fluid inside the gearbox housing was studied. A simple-stage helical gear system was considered. The housing

having parallelepiped form was made of five rigid panels (rigid part), and one elastic panel on which the driving and driven shafts were mounted. The dynamic response of the gearbox for different rotational speed was computed from the recovered surface acceleration of the housing. The predictions of the radiation acoustic field and the pressure envelope were obtained by using Rayleigh integral (RI) method. Numerical results showed that the acoustic field depends only on the geometrical dimensions and the vibrational distribution of the elastic face, but also on the resonance frequencies of the whole gearbox [6].

The above review has shown that almost the efforts which had been done in the subject was directed towards the studying the basic vibration and interior noise generation of gearboxes theoretically considering single-stage gearbox. Their contributions were limited due to the consideration of meshing stiffness as the only source of excitation and ignoring the other sources. In addition, the radiation efficiency has been ignored, whereas experimental studies have given little considerations. Exterior noise radiation has also given little attention particularly that concerned with original vehicle gearbox. However, the objective of this paper is to develop a method for predicting the contributions to exterior noise radiated by an original vehicle gearbox structure using measured vibration response, considering all the sources exist taken the radiation efficiency into consideration.

2. RELATIONSHIP BETWEEN SURFACE VIBRATION AND RADIATED NOISE

2.1 Sound Power Theory

The theory of sound power radiated by a vibrating surface is dependent on the following parameters [7]:

- Velocity response of the vibrating surface
- The coupling coefficient between the vibrating surface and the surrounding space
- The surface area of the vibrating surface.

The equation relating these parameters is,

$$W_{rad} = W_{vib}.\sigma = \rho.C.A.\overline{V}^2.\sigma \tag{1}$$

States that the radiated acoustic power is dependent on the product of vibratory power in the surface and the efficiency with which power is transferred from the surface to its surrounding. For free fields conditions,

$$W_{rad} = I * S \tag{2}$$

$$I = P^2 / \rho * C \tag{3}$$

Substituting for W_{rad} in equation (1) and transposing, the space averaged sound pressure level (SPL) can be obtained as

$$P^2 = \rho^2 * C^2 * .\overline{V}^2 * \sigma * A * S^{-1} \tag{4}$$

Equation (4) determines the mean square space average SPL, that SPL which be expected at any point on a hypothetical surface in space at a given distance "r" from the source. The distance "r" must be at least equal to 0.6 meters to avoid the near field effects. This is assuming that the source is radiating sound uniformally from its surface.

2.2 The Radiation Efficiency

The radiation efficiency (σ) which is presented in equation (4) can be established for the surface of a gearbox structure by idealizing the structure as an assembly of simple flat plates (panels) as shown in Fig. 1. This idealization has been chosen because there is evidence that parts of the gearbox do vibrate in a plate like manner and because there is available analytically derived data on radiation efficiency obtained by [8]. The details of estimated the individual plate in the idealization is presented in APPENDIX.

To calculate the radiation efficiency of a set of plates (panels). It is necessary now to account for the effect of each panel has on the sound radiated by the whole set. For this calculation the panels are considered as independent panels with surface areas a_1, a_2, a_3,..., a_n $A = \sum_{i=1}^{i=n} a_i$ is the total surface area of the set of panels. Therefore, the proportional effect on the radiation efficiency of the i^{th} panel on that of the whole set is given by $\sigma_i . a_i /A$. The radiation efficiency of the set therefore being

$$\sigma_T = \sum_{i=1}^{i=n} \sigma_i * \alpha_i \tag{5}$$

Where $\alpha_i = a_i / A$

Now, since (σ) is a quantity which varies with frequency as well as plate size, it is convenient to represent this in matrix form for calculation, thus.

$$\begin{bmatrix} \sigma_{11} \ldots\ldots\ldots \sigma_{12} \ldots\ldots\ldots \sigma_{1n} \\ \sigma_{21} \ldots\ldots\ldots \sigma_{22} \ldots\ldots\ldots \sigma_{2n} \\ .\sigma_{m1} \ldots\ldots\ldots \sigma_{m2} \ldots\ldots\ldots \sigma_{mn} \end{bmatrix} \begin{bmatrix} \alpha_1 \\ \alpha_2 \\ \alpha_n \end{bmatrix} = \begin{bmatrix} \sigma_{T1} \\ \sigma_{T2} \\ \sigma_{Tm} \end{bmatrix} \tag{6}$$

$$\underline{\sigma} * \underline{\alpha} = \underline{\sigma}_T \tag{7}$$

Where $\underline{\sigma}$ is the matrix of m frequency rows and n panel (plate) columns, and $\underline{\alpha}$ is the vector of n panel area ratio (a_n/A).

2.3 The Vibration Response

The velocity response of the vibrating surface ($\overline{V}$) which appears in equation (4) cannot be expressed by a simple mathematical function. This means that this velocity needs to be measured. However, based on analysis, any structure has to be idealized as a set of

independent plates (panels), for each of which an average vibration velocity can be determined. Therefore, the accuracy of the predicted sound pressure level (SPL) based on this theory will be limited by the number of structure panels used in idealization. Hence, the bigger is the number of panels, the more accurate will be the prediction of SPL resulting from the overall structure panels or part of it. The vibration velocity measurements must include narrow, 1/3 octave and RMS spectra form, when the RMS vibration velocity response $\langle \bar{V}_T \rangle$ of each area represented by a panel in the idealization has been measured in the octave spectrum form. The matrix solution can be applied to obtain the overall vibration velocity response spectrum for the structure represented by a set of panels.

To calculate the overall vibration velocity response of a set of panels, it is necessary to account for the effect of each panel has on the vibration velocity produced by the whole set. For this calculation, the proportional effect of the vibration velocity response of the i th panel on that of the whole set can be given by $\langle \bar{V}_T \rangle . a_i \ / A$. The vibration velocity of the set therefore being:

$$\langle V_T \rangle = \sum_{i=1}^{i=n} \langle \bar{V}_i \rangle * \alpha_i \tag{8}$$

Now, since ($\bar{V}$) is a quantity which varies with frequency as well as plate size, it is convenient to represent this in matrix form similar to equation (6).

$$\underline{\bar{V}} * \alpha = \langle \underline{\bar{V}} \rangle_T \tag{9}$$

Having obtained values of σ_T and $\langle \overline{V} \rangle_T$ from structure idealization and vibration velocity response measurement, and a value for AS^{-1} from a knowledge of structure surface area and acoustic field idealization, equation (4) can be used to obtain 1/3 octave SPL either in dB or in dB(A)

3. EXPERIMENTAL METHODOLOGY

3.1 Experimental Setup

The experimental setup is used for the vehicle gearbox manual transaxle system considered in this work. The vehicle gearbox manual tramsaxle (constant mesh) system shift gears are tabulated in Table 1. The entire system is settled in an oil basin in order to ensure proper lubrication. SAE 75W-90 oil (ESSO Gear Oil GX) was used as a standard lubricant oil type. The full lubrication level is 100 mm and half lubrication level is 50 mm. The lubricant oil type specifications are listed in Table 2. The gearbox was powered by the electric motor and consumes its power on a hydraulic disc brake. A short shaft of 20 mm diameter was attached to the shaft of the motor through a flexible coupling. This was to minimize effects of misalignment and transmission of vibration from the motor. The shaft is supported at its ends through two ball bearings and then the motion is transmitted directly to the gearbox. The system is illustrated schematically in Fig. 1, where a photograph for the gearbox used in this work is shown in Fig. 2.

Table 1. Manual transaxle system specifications

S/No.	Model		M5EF2
1	Type		Helical gears - forward 5 speed, reverse 1 speed
2	Engine displacement		1.1 MPI engine
		First	3.545
		Second	1.894
		Third	1.192
3	Gear ratio	Forth	0.853
		Fifth	0.719
		Reverse	3.636
4	Final gear ratio		4.437

Table 2. Oil type lubricant specifications

S/No.	SAE Grade	SAE 75W-90	Remarks
1	Viscosity Index	177	
2	Flash Point, COC: ºC	170	
3	Pour Point ºC	-42	
4	Kinematic viscosity@40ºC	92.6	
5	Kinematic viscosity@100ºC	15.4	
6	Density@ 15ºC	875	

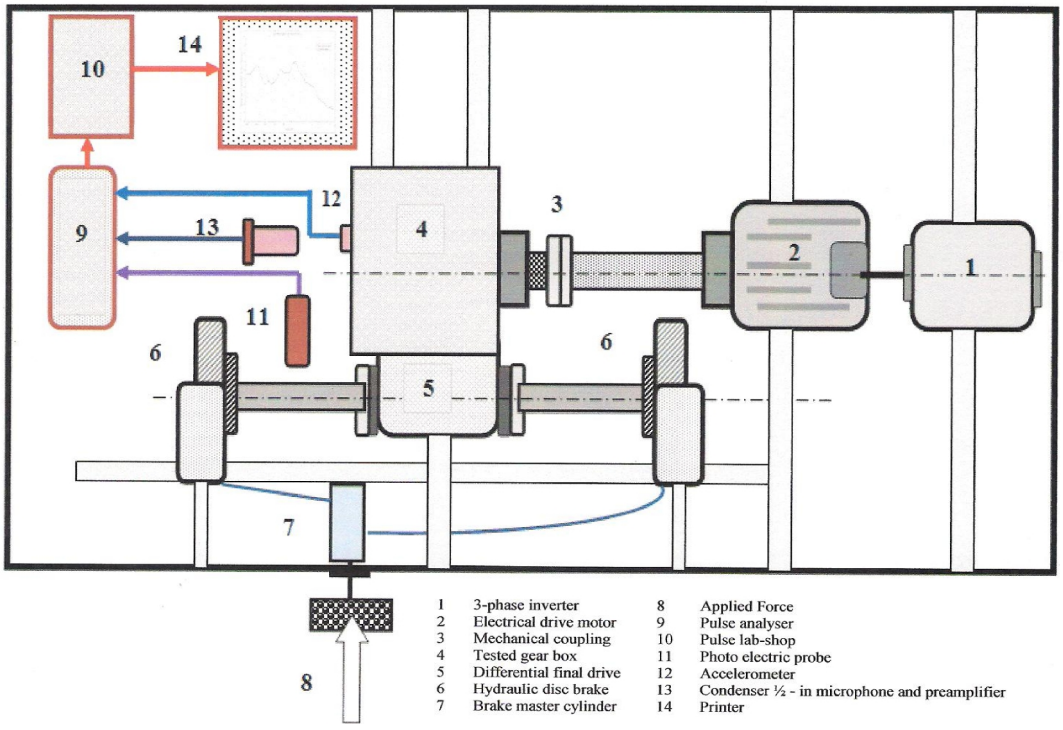

Fig. 1. Test rig schematically layout

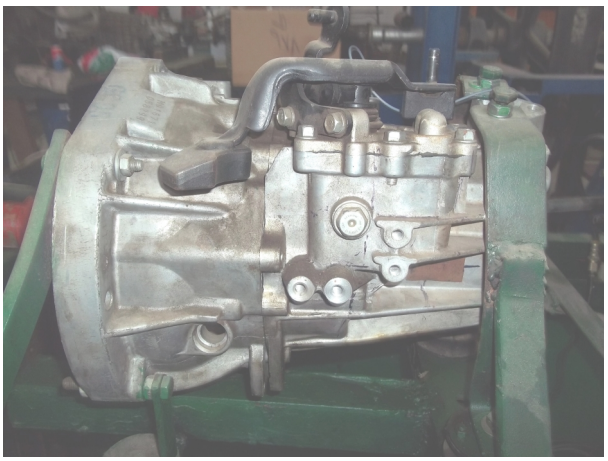

Fig. 2. Original vehicle gearbox

3.2 Test Procedure

Prior to testing, the gearbox had been separated from its vehicle and put on a heavy steel stand made; and mounted on it. The reason for doing this was to measure the gearbox structure response away from other vehicle elements (tire/road interface, engine, etc) not only, but also to allow the gearbox structure, to be tested with and without loads at different speed conditions. The vibration velocity responses for the gearbox structure were measured by accelerometers which had been mounted on the center of each panel and element surface. The type of the accelerometers is B&K 4514-B-001, where their mounted resonant frequency is 32 kHz, transverse resonant frequency is 29.9 kHz, frequency range is 1 Hz-10 KHz and weight is 8.7 grams. Based on the accelerometers specifications stated previously, their readings were not affected. The accelerometer signals were recorded and were passed to the data analysis system analyzer (PULSE labshop and PULSE analyzer). At the same time the gearbox exterior noise in terms of sound pressure level were measured by 1/2 in microphone placed at mainly four points around the gearbox structure areas (right hand side, top, Left hand side and rear) away from the gearbox structure by 0.6 m **{1}**. The microphone signals were passed to the data analysis system analyzer as in vibration velocity measurements. The motor speed was measured by photoelectric tachometer probe which placed in front of the gearbox input shaft and its signals passed to the data analysis system. Also, the torque load was computed by using the measured oil pressure on vehicle wheel axle and transferred to the gearbox through the reduction ratio for the differential and gearbox with the dimensions of the brake master cylinder and brake disc. The motor speed was varied up to 1000 rpm, torque load is 12 Nm and the frequency range is 2000 Hz.

4. PREDICTION PROCEDURE DETAILS

The idealization of the vehicle gearbox structure panels and elements used in this work is shown in Fig. 3, where four major panels are considered, i.e. right hand side (R.H.S), top, left hand side (L.H.S) and rear. Each of which is divided into 4 elements areas. The panels and elements dimensions are shown in the figure, while the physical properties and end conditions are tabulated in Table 3, from which the fundamental modes (natural frequency) were computed based on equation (A.1), APPENDIX. Consequently, the values of the normal modes radiation efficiency (σ) for the idealized panels and elements were calculated

according to equation (6). The gearbox structure obviously, has many modes of vibration, and it would be important critical to attempt to define the all to find the position of maximum response for each mode. When the response ($\overline{V}$) of each area represented by a panel in the idealization has been calculated in octave band spectrum form, the matrix solution presented in equation (9) was applied to obtain the response spectrum for an area of the whole gearbox structure represented by a set of panels. This can account the effect of each panel has on the vibration velocity response produced by whole set.

Table 3. Physical properties of the vehicle gearbox panels 1

Panel no.	Description		Young's modulus (E), $N/m^2 \times 10^{-10}$	Panel material density (ρ_p), kg/m^3	Material poisson's ratio (ν)	Edge (end) conditions	
	Panel name	Element no.				X	Y
	Right	1	7.1	2700	0.33	s	c
1	hand	2	7.1	2700	0.33	c	c
	side	3	7.1	2700	0.33	s	c
		4	7.1	2700	0.33	c	c
		5	7.1	2700	0.33	s	c
2	Top	6	7.1	2700	0.33	c	c
		7	7.1	2700	0.33	s	c
		8	7.1	2700	0.33	c	c
	Left	9	7.1	2700	0.33	s	c
3	hand	10	7.1	2700	0.33	c	c
	side	11	7.1	2700	0.33	s	c
		12	7.1	2700	0.33	c	c
		13	7.1	2700	0.33	c	c
4	Rear	14	7.1	2700	0.33	c	c
		15	7.1	2700	0.33	c	c
		16	7.1	2700	0.33	c	c

s- Simply support; c- clamped (fixed) support.

Accordingly, when a surface in the gearbox structure at a discrete frequency and with a predictable mode shape, it is possible to calculate the sound pressure level (SPL) at a point above the surface. This calculation was achieved by using equation (4). Even so, a considerable amount of date is necessary to quantify the behavior of gearbox structure over a limited frequency band. The use of these analytical techniques on complex structure such as vehicle gearbox is completely precluded by the enormity of the calculation. However, by considering the total power radiated rather than pressure at discrete points, and by considering the use of 1/3-octave bands rather than discrete frequencies, it is possible to obtain a considerable reduction in the calculation effort.

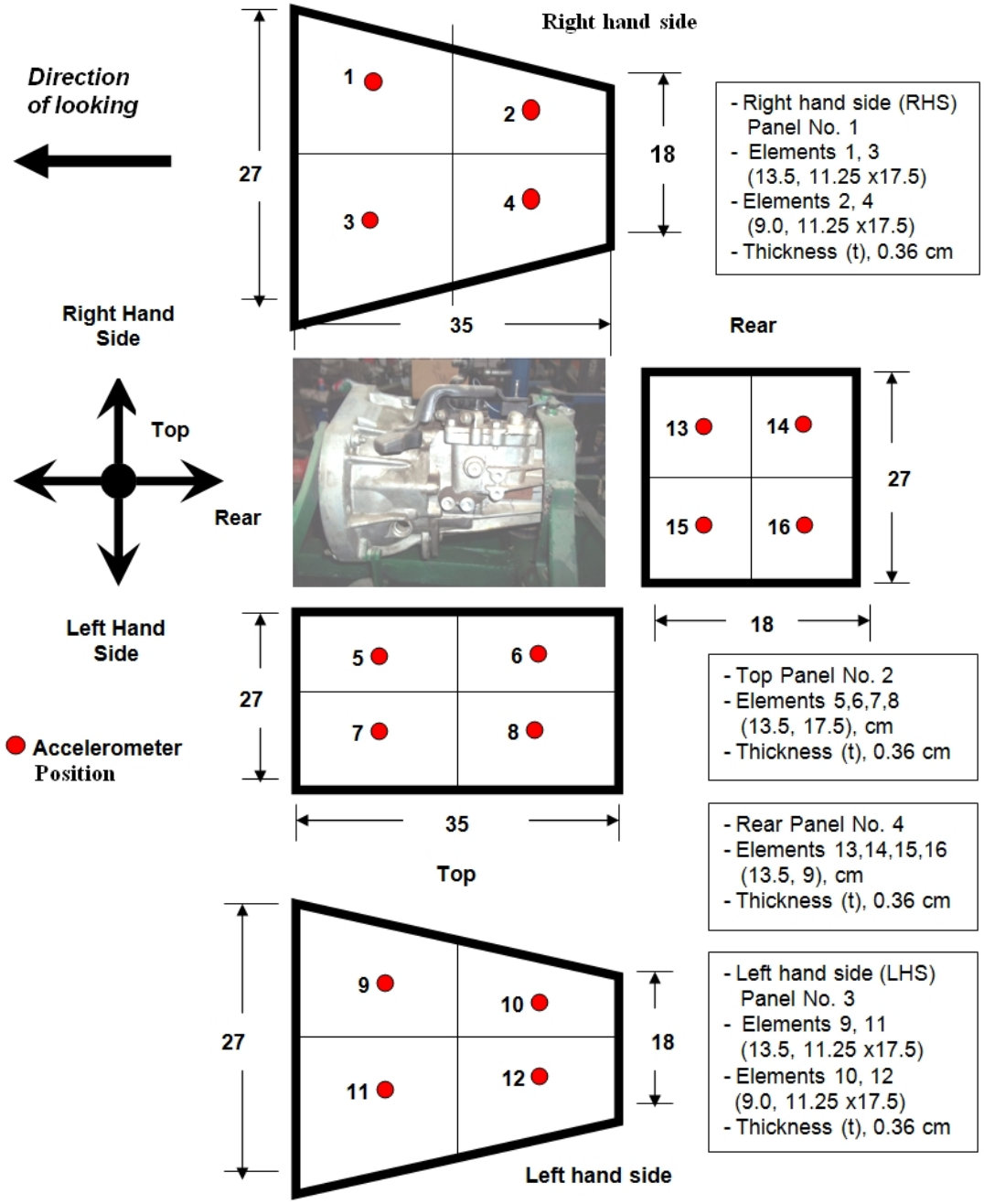

Fig. 3. Idealization of vehicle gearbox structure as a set of structure elements

5. RESULTS AND DISCUSSION

Sample from the measured sound pressure level (SPL) in the form of narrow and 1/3-Octave bands for right hand side (R.H.S) panel at point of 0.6 m away from the gearbox structure are shown in Figs. 4 and 5 respectively. The data present in Fig. 5 will be used later for the

comparison between the predicted and measured SPL. Figs. 6 and 7 show samples from the vibration velocity responses in the form of narrow and 1/3-Octave bands for element No.1 respectively.

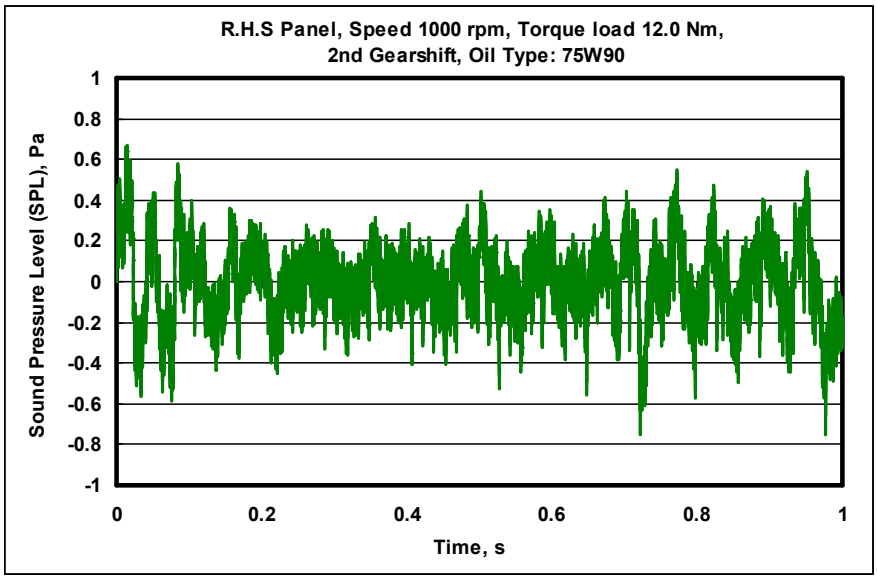

Fig. 4. Time history (domain) of sound pressure level measured for R.H.S. panel

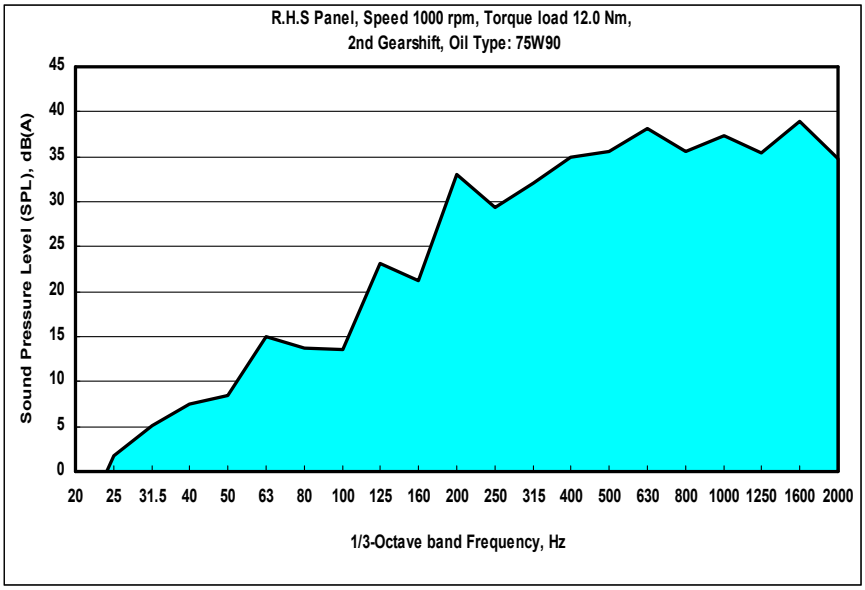

Fig. 5. 1/3-Octave band sound pressure level measured for R.H.S. panel

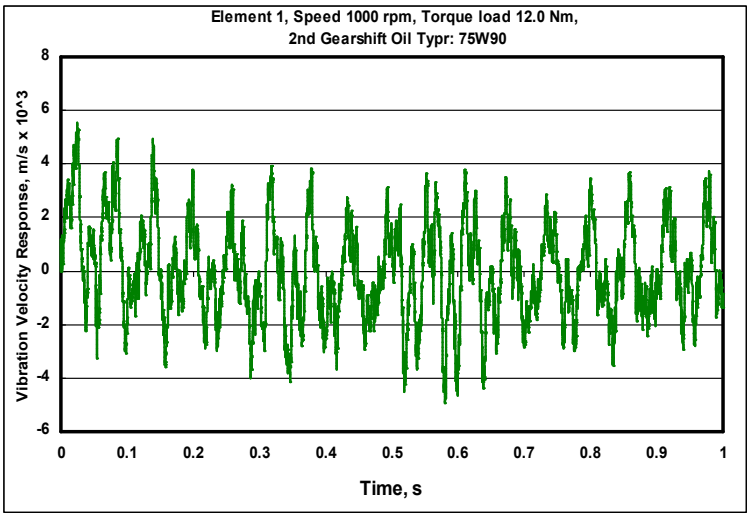

Fig. 6. Time history (domain) of measured vibration velocity for element 1

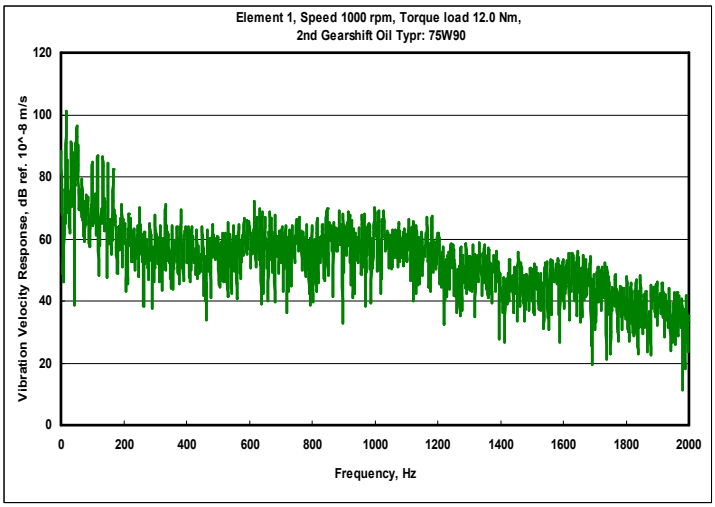

Fig. 7. Frequency domain of measured vibration velocity for element 1

Figs. 6 and 7 show the time-history and frequency domain spectra of the measured vibration velocity for element No. 1 in the sub-critical range of angular speeds i.e. teeth mesh frequencies. The gear mesh frequency corresponding to the motor speed of 1000 rpm and input gear number of teeth is 26 was computed based on this relation, f_m= (motor speed * number of teeth of the output gear)/ 60, where f_m is the fundamental gear mesh frequency. This gives value of f_m = 434 Hz and is located with its sub-harmonics within the frequency range of 2000 Hz. The value of f_m is significantly higher than the resonance frequencies of the gearbox structure. The vibration velocity levels are being higher for the resonance frequencies than that for fundamental gear mesh frequency.

5.1 Various Elements Measured Vibration Velocity

Figs. 8 to 11 show the 1/3-octave band averages of the measured vibration velocity responses spectra (m/s) at the centers for all the elements individually which are considered in the gearbox structure idealization. The gearbox structure has to be spitted into four major panels. Each major panel has four individual elements areas as shown in Fig. 3. The four panels are right hand side (R.H.S), top, left hand side (L.H.S) and rear. The motor speed is being 1000 rpm and torque load is 12 Nm, while the oil type is SAE 75W90 (Table 2). It is observed from these figures that the measured vibration velocity responses varies from element to another, where some peaks are existed almost in all the gearbox structure elements up to 1/3-octave frequency of 400 Hz. Furthermore, the vibration velocity level is different from element to another due to the element location in the idealization, its area and end conditions.

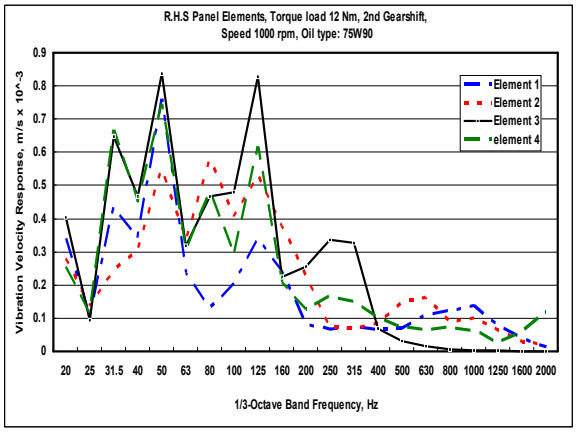

Fig. 8. 1/3-Octave band vibration velocity measured at the center of R.H.S panel elements

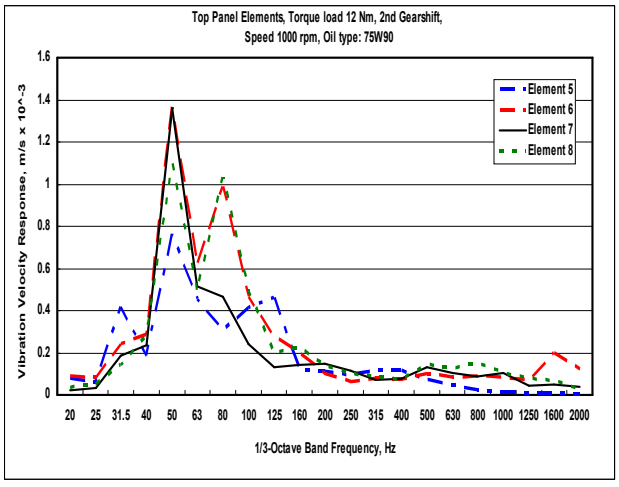

Fig. 9. 1/3-Octave band vibration velocity measured at the center of top panel elements

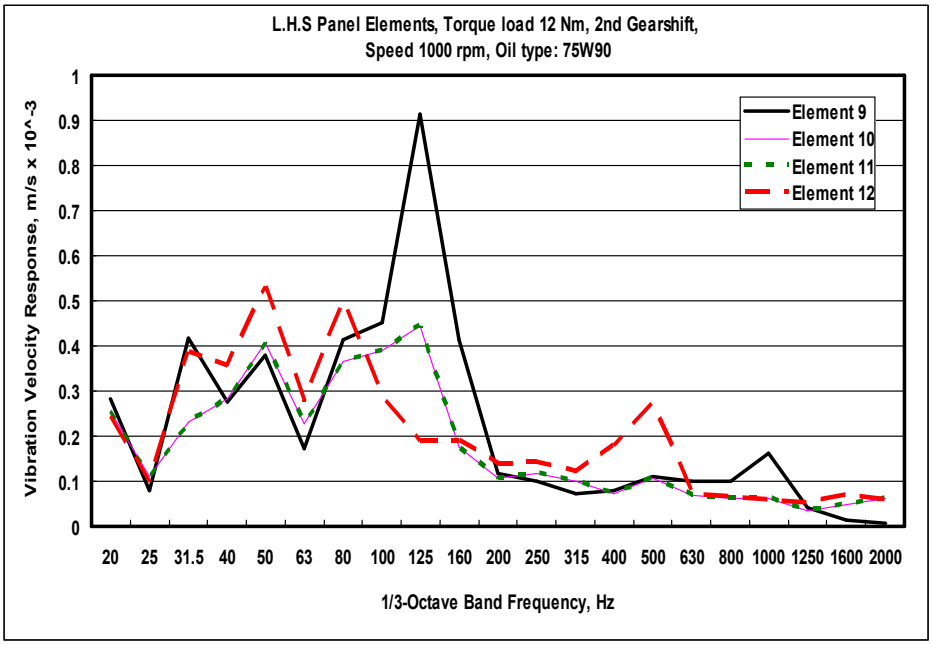

Fig. 10. 1/3-Octave band vibration velocity measured at the center of L.H.S panel elements

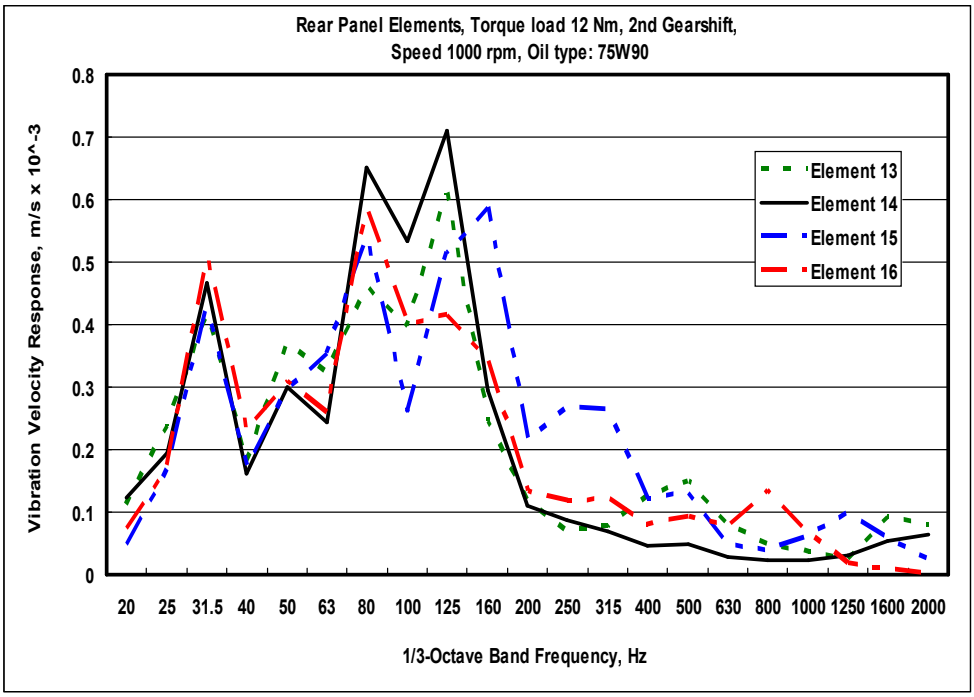

Fig. 11. 1/3-Octave band vibration velocity measured at the center of rear panel elements

Fig. 12 shows the overall RMS values for the individual element, where element No. 3 (R.H.S-panel) has the highest vibration velocity response followed by element No. 6 (top-panel), element No. 9 (L.H.S-panel) and element No. 15 (rear-panel).

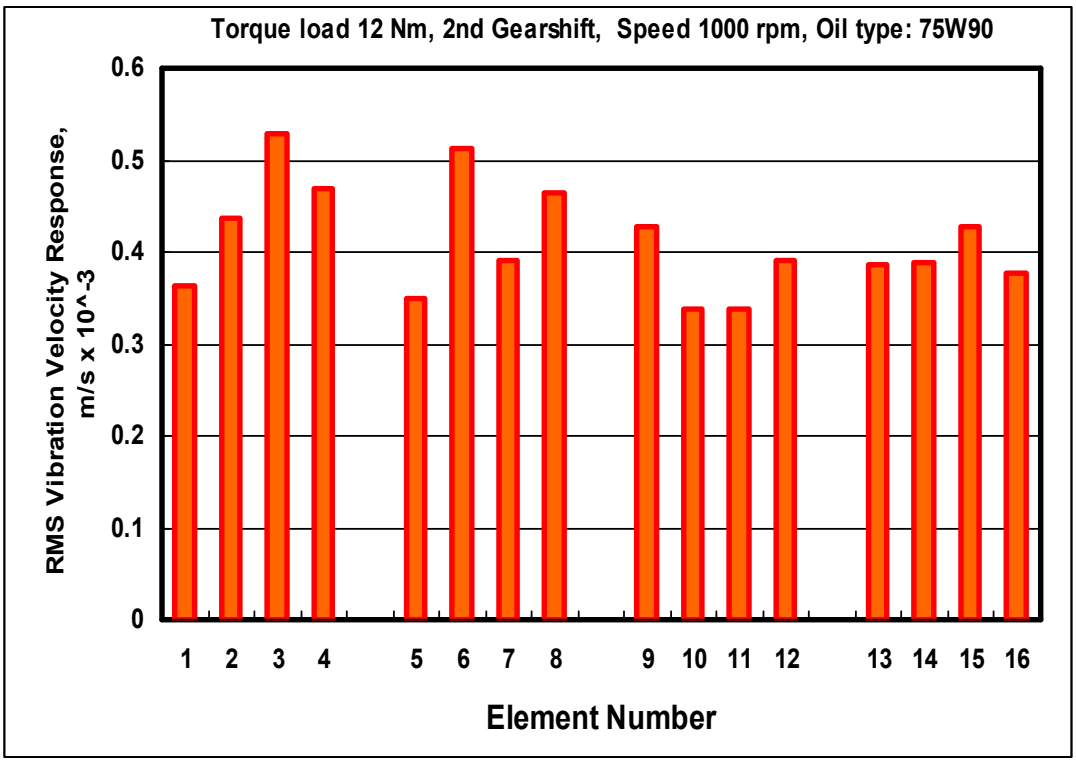

Fig. 12. Overall RMS vibration velocity calculated for all the gearbox structure elements

5.2 Gearbox Structure Panels Radiation Efficiency

The radiation efficiencies for the individual panels of the vehicle gearbox structure which are considered in the idealization along with the overall averages and are presented in Table 4. The gearbox surface is partitioned as four major panels. Each major panel has four individual elements areas as shown in Fig. 3. The overall averages of the radiation efficiency for the individual elements are shown in Fig. 13, where the radiation efficiencies for the individual elements in each major panel have an equal value. This is true, where all the elements in any major panel are equal in area.

Table 4. Predicted radiation efficiency (σ) of manual gearbox structure panels elements

P. N	R.H.S				TOP				L.H.S				REAR			
El. N	1	2	3	4	5	6	7	8	9	10	11	12	13	14	15	16
F. B																
20	0.0006	0.0008	0.0008	0.0007	0.0007	0.001	0.001	0.001	0.0006	0.001	0.001	0.0008	0.0007	0.0007	0.0007	0.0007
25	0.0007	0.0009	0.0009	0.00075	0.0008	0.0008	0.001	0.00075	0.0007	0.001	0.001	0.0009	0.00075	0.00075	0.00075	0.00075
31.5	0.0008	0.002	0.002	0.0008	0.0008	0.0008	0.001	0.0008	0.0008	0.002	0.001	0.002	0.0008	0.0008	0.0008	0.0008
40	0.0095	0.004	0.004	0.0009	0.0009	0.0009	0.001	0.0009	0.00085	0.004	0.001	0.004	0.0009	0.0009	0.0009	0.0009
50	0.0025	0.005	0.005	0.001	0.0025	0.0025	0.003	0.0025	0.0025	0.005	0.003	0.005	0.001	0.001	0.001	0.001
63	0.003	0.0055	0.0055	0.0025	0.004	0.004	0.004	0.004	0.003	0.006	0.003	0.0055	0.0025	0.0025	0.0025	0.0025
80	0.005	0.006	0.006	0.0065	0.005	0.005	0.005	0.005	0.005	0.006	0.005	0.006	0.0065	0.0065	0.0065	0.0065
100	0.007	0.007	0.007	0.008	0.0075	0.0075	0.0075	0.0075	0.007	0.007	0.007	0.007	0.008	0.008	0.008	0.008
125	0.008	0.008	0.008	0.009	0.0085	0.0085	0.0085	0.0085	0.008	0.008	0.008	0.008	0.009	0.009	0.009	0.009
160	0.01	0.01	0.01	0.01	0.03	0.03	0.03	0.03	0.01	0.01	0.01	0.01	0.01	0.01	0.01	0.01
200	0.045	0.035	0.035	0.05	0.05	0.05	0.05	0.05	0.045	0.035	0.045	0.035	0.05	0.05	0.05	0.05
250	0.06	0.05	0.05	0.06	0.065	0.065	0.065	0.065	0.06	0.05	0.06	0.05	0.06	0.06	0.06	0.06
315	0.065	0.053	0.053	0.07	0.07	0.07	0.07	0.07	0.065	0.053	0.065	0.053	0.07	0.07	0.07	0.07
400	0.068	0.056	0.056	0.075	0.075	0.075	0.075	0.075	0.068	0.056	0.068	0.056	0.075	0.075	0.075	0.075
500	0.07	0.06	0.06	0.08	0.08	0.08	0.08	0.08	0.07	0.06	0.07	0.06	0.08	0.08	0.08	0.08
630	0.085	0.07	0.07	0.09	0.085	0.085	0.085	0.085	0.085	0.07	0.085	0.07	0.09	0.09	0.09	0.09
800	0.09	0.08	0.08	0.1	0.09	0.09	0.09	0.09	0.09	0.08	0.09	0.08	0.1	0.1	0.1	0.1
1000	0.095	0.09	0.09	0.13	0.095	0.095	0.095	0.095	0.095	0.09	0.095	0.09	0.13	0.13	0.13	0.13
1250	0.097	0.093	0.093	0.4	0.097	0.097	0.097	0.097	0.097	0.093	0.097	0.093	0.4	0.4	0.4	0.4
1600	0.098	0.095	0.095	0.5	0.098	0.098	0.098	0.098	0.098	0.095	0.098	0.095	0.5	0.5	0.5	0.5
2000	0.1	0.1	0.1	0.6	0.1	0.1	0.1	0.1	0.1	0.1	0.1	0.1	0.6	0.6	0.6	0.6
Aver.	0.076	0.083	0.075	0.200	0.200	0.083	0.076	0.200	0.200	0.083	0.076	0.083	0.088	0.088	0.088	0.088

P. N.: Panel name El. N. : Element Number F. B.: Frequency 1/3-octave band, Hz

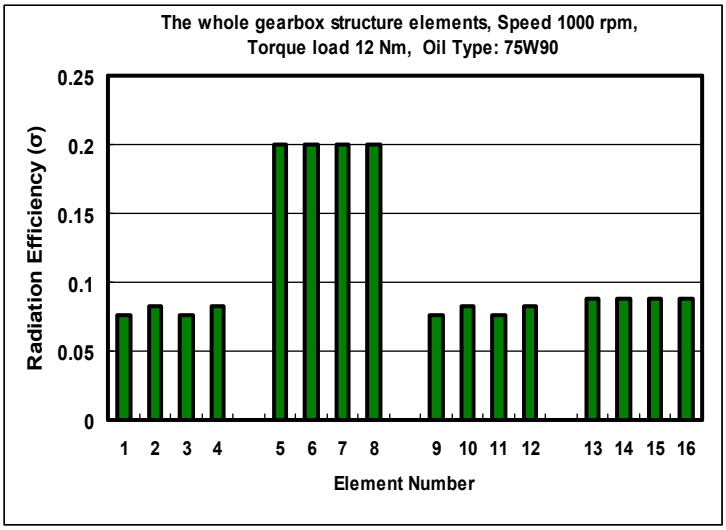

Fig. 13. Overall average of radiation efficiency calculated for all the gearbox structure elements

5.3 Comparison between Measured and Predicted SPL

Having calculating the whole average radiation efficiency and the whole RMS vibration velocity for the R.H.S panel based on equations (6) and (9) respectively. Their results are plotted in Figs. 14 and 15 respectively The motor speed is being 1000 rpm with torque load of 12 Nm and oil type of SAE 75W90.

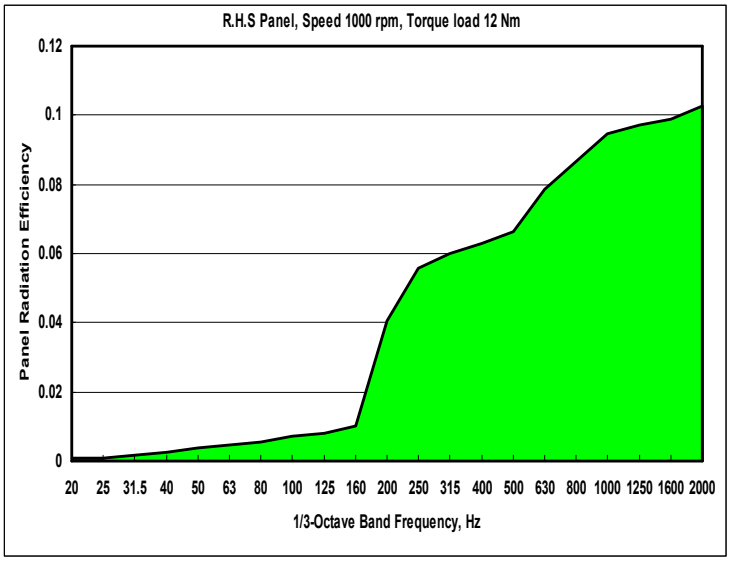

Fig. 14. The whole average radiation efficiency calculated for the R.H.S panel

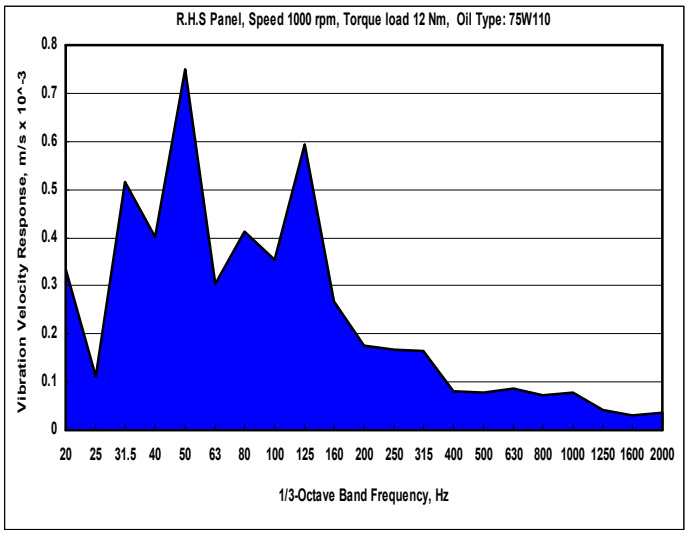

Fig. 15. The whole RMS vibration velocity calculated for the R.H.S panel- Oil type SAE 75W90

Fig. 16 shows the comparisons between 1/3-octave bands spectra predicted sound pressure level (SPL) in dB (A) computed based on equation (4) and those measured for right hand side (R.H.S) panel at point of 0.6 m away from the gearbox structure. The predicted SPL spectrum is slightly higher than that for the measured spectra particularly over 1/3-octave of 250 Hz (Fig. 16). The fit of the predicted to the measured is not quite as close as expected but this is still acceptable. It is observed that the SPL can be predicted within 3 dB (A) of the measured level in each 1/3-Octave band. The SPL is expressed by dB (A) reference to 20 x 10^{-5} N/m^2.

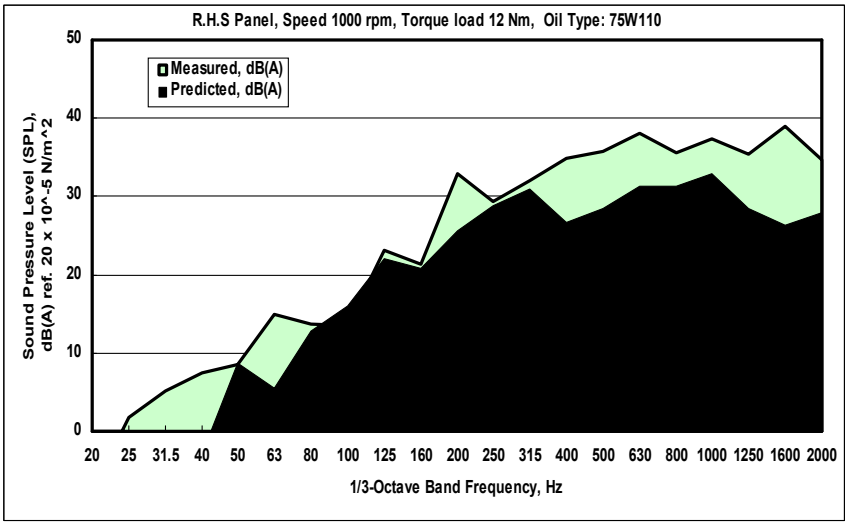

Fig. 16. Comparison between measured and predicted SPL calculated the R.H.S panel- Oil type SAE 75W90

5.4 Various Elements Noise Sources Contribution

The elements noise sources contributions from the gearbox structure elements considered in this study were predicted individually based on equation (4) at point of 0.6 m away from the gearbox structure sides in terms of SPL, dB (A), and are shown in Figs. 17 and 20. The gearbox structure has to be spitted into four major panels. The motor speed is being 1000 rpm without load and oil type of SAE 75W90. It can be seen from these figures that the predicted SPL varies from element to another, where some peaks are existed almost in all the gearbox structure elements spectra due to the element location in the idealization, its area and its edge (end) conditions. Fig. 21 shows the overall RMS values for the individual element, where element No. 11 (L.H.S-panel) has the highest sound pressure level response followed by element No. 5 (top-panel) and element No. 7 (top-panel).

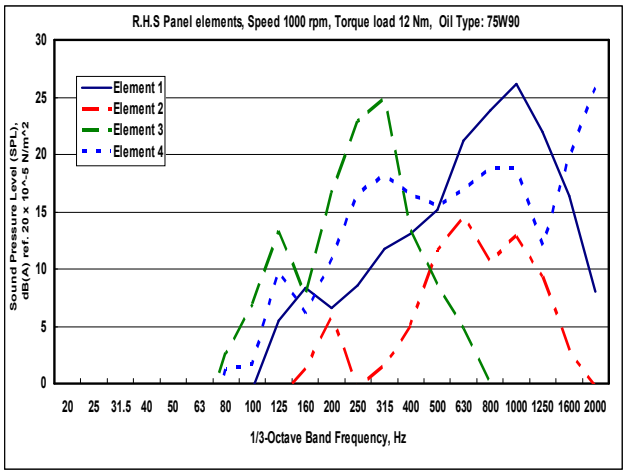

Fig. 17. 1/3-Octave band sound pressure level (SPL) predicted in front of the center of panel R.H.S elements

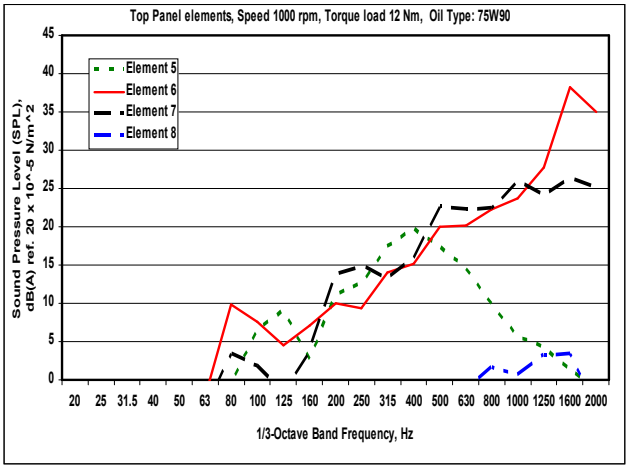

Fig. 18. 1/3-Octave band sound pressure level (SPL) predicted in front of the center of top panel elements

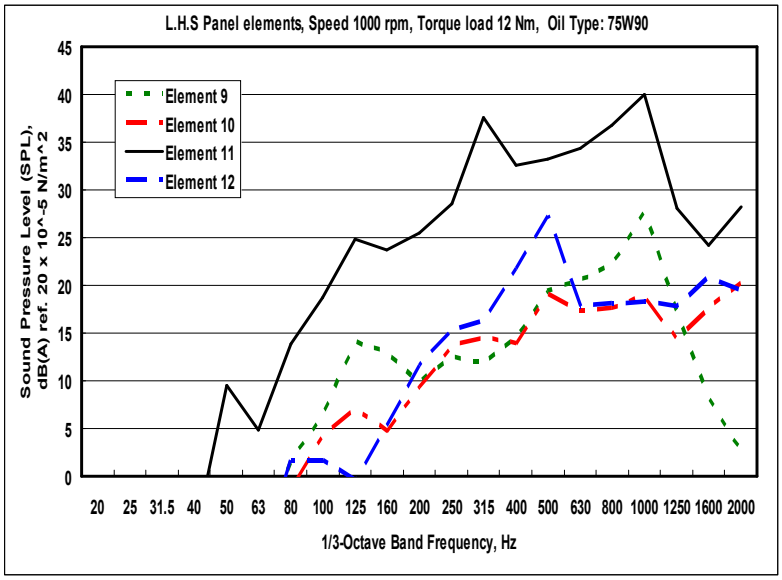

Fig. 19. 1/3-Octave band sound pressure level (SPL) predicted in front of the center of L.H.S panel elements

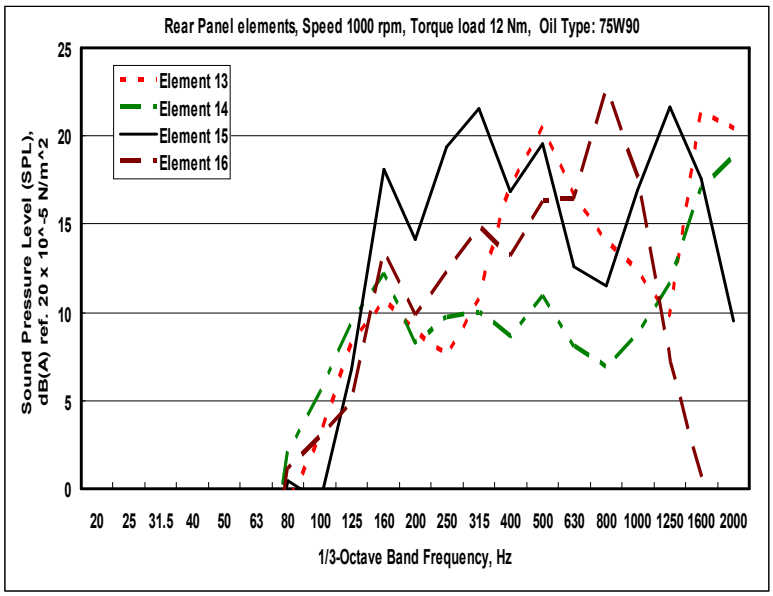

Fig. 20. 1/3-Octave band sound pressure level (SPL) predicted in front of the center of rear panel elements

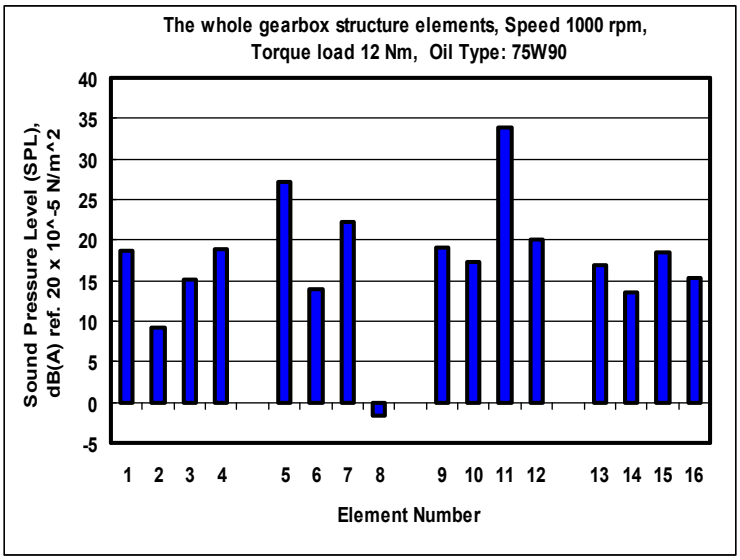

Fig. 21. Overall RMS sound pressure level (SPL) predicted for all the gearbox structure elements

6. CONCLUSIONS

1. It has been shown that the noise in terms of sound pressure levels can be predicted to within 3 dB (A) of those measured levels. Moreover, a reliable method of ranking the noise sources based on the idealization technique and vibration measurements has been developed which removes much of the uncertainty from noise reduction exercise.

2. The radiation efficiency of the vehicle gearbox surface can be calculated from an idealization of the gearbox surface as a set of independent vibrating panels, without using microphone measurements.

3. The calculation procedure tends itself to being fully computerized and providing that the idealization and test are carefully designed, reliable frequency analysis can be achieved. Furthermore, the measurements and analysis procedures presented in this work can be applied on any structure, if the major noise sources need to be identified and treated.

4. The potentially noisy surface areas forming the vehicle gearbox structure have been identified, where the overall RMS values for the individual element show that the element No. 11 (L.H.S-panel) has the highest sound pressure level response followed by element No. 5 (top-panel) and element No. 7 (top-panel).

COMPETING INTERESTS

Authors have declared that no competing interests exist.

REFERENCES

1. Chen Y, Ishibashi A. Investigation of the Noise and Vibration of Planetary Gear Drives. Gear Technology. January/February; 2006.
2. De Souza LTS, Caldas IL, Viana RL, Batista AM, Kapitaniak T. Noise-induced Basin Hopping in a Gearbox Model Chaos, Solitons and Fractals. 2005;26:1523-1531.
3. Barthod M, Hayne B, Te´bec JL, Pin JC. Experimental Study of Dynamic and Noise Produced by a Gearing Excited by a Multi-Harmonic. Applied Acoustics. 2007;68:982-1002.
4. Bozca M. Torsional Vibration Model Based Optimization of Gearbox Geometric Design Parameters to Reduce Rattle Noise in an Automotive Transmission. Mechanism and Machine Theory. 2010;45:1583-1598.
5. Agemi FM, Ognjanovi M. Gear Vibration in Supercritical Mesh-Frequency Range. Faculty of Mechanical Engineering (FME, Belgrade, Transactions. 2004;32:87-94.
6. Abbes M S, Bouaziz S, Chaari F, Maatar M, Haddar M. An Acoustic Structural Interaction Modeling for the Evaluation of a Gearbox-radiated Noise. International Journal of Mechanical Science. 2008;50:569-577.
7. Bruce RD. Field Measurements: Equipment and Techniques. Noise and Vibration Control. (Edited by L. Beranek). 74-99, Graw-Hill; 1971.
8. Wallance CE. Radiation Resistance of a Rectangular Plate" Journal of the Acoustical Society of America. 1972;51(3):949.
9. Szchenyi CA. Approximate Methods for Determination of Natural frequencies and Normal Modes of Stiffened Flat and Curved plates. Presented in. Current Developments in Sonic Fatigue. a conference held at ISVR, University of Southampton, 1970;6-9th July.

APPENDIX

Radiation Efficiency Estimation

The fundamental modes can be calculated from an approach based on the Reyleigh Ritz classical analysis. This approach contains modal frequencies for simply support rectangular plate as shown in Fig. A.1 using the following equation:

$$F_{m,n} = \{\sqrt{E*t^2/[\rho_p*(1-v^2)*12]}\}*\{(m*\pi/a)^2+(n*\pi/b)^2\} \quad (A.1)$$

In practical this is not always the case. Other boundary conditions (clamped or fixed) must be applied using the method described in [9], where values $F_{m,n}$ for clamped edge plates can be obtained as following:

- For a plate clamped on both edges in 'x' direction

$$\bar{b} \Rightarrow (\frac{1.05*n}{n+0.5})*b \quad (A.2)$$

- For a plate clamped on both edges in 'y' direction

$$\bar{a} \Rightarrow (\frac{1.05*m}{m+0.5})*a \quad (A.3)$$

The values of the radiation efficiency (σ) for various modes of vibration of a simply supported rectangular plate were derived by [9]. The simplification to Wallace's radiation efficiency curves could be made for third octave analysis. This work showed that calculated values were at least as accurate as measured results for radiation efficiency because the third octave filtering effectively merges the radiation efficiency of modes within third octave band. This simplification reduces the curves to one for the fundamental mode and one for the average of all other modes. Those curves are plotted against the non-dimensional wave number ratio (γ) as shown in Fig. A.2. The ratio (γ) is defined as follows:

(γ) = (acoustic wave number)/(structure wave number) = K / K_p (A.4)

Where $K=(F_{m,n})/C$ and $K_p = [(m*\pi/a)^2+(n*\pi/b)^2]^{1/2}$ (A.5)

The relationship between wave number ratios at the fundamental mode frequency ($f_{1,1}$) and any other frequency for a simply supported rectangular plate is well documented in **[10]**. This shows that the wave number ratio for 1/3 octave band ($\gamma_{\Delta c}$) whose centre frequency is ($f_{\Delta,c}$) is given by,

$$\gamma_{\Delta c} = (F_{\Delta c}/F_{1,1})^{1/2} * \gamma_{1,1} \quad (A.6)$$

Using equation (3.10), and the curves of Fig. A.2, the predicted radiation efficiency of each plate considered can be determined

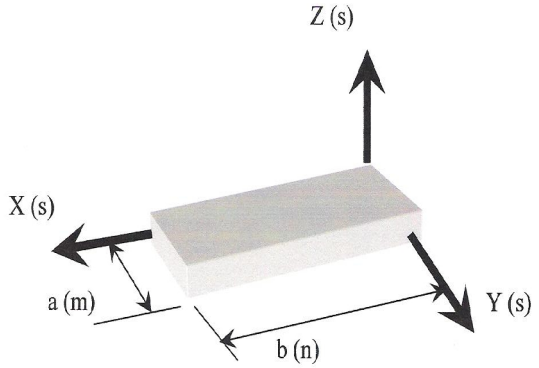

Fig. A.1. Simple support

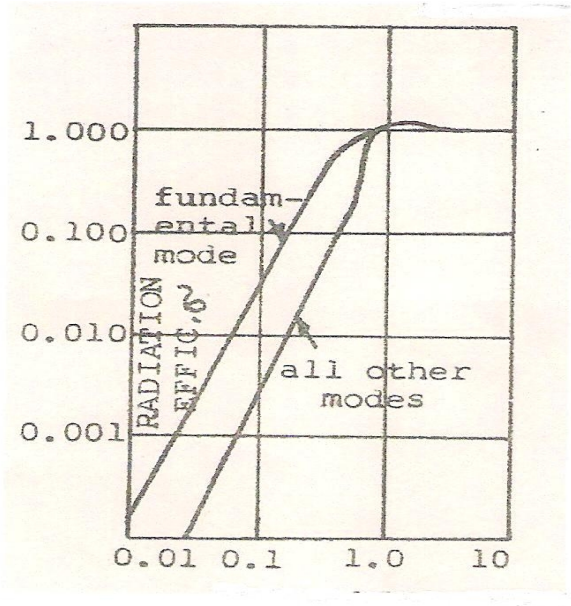

Fig. A.2. Radiation efficiency as a function

Peer-review history:
The peer review history for this paper can be accessed here:
http://www.sciencedomain.org/review-history.php?iid=226&id=5&aid=1439